Inorganic Chemistry

ARTICLE

pubs.acs.org/IC

Effect of the Addition of a Fused Donor−Acceptor Ligand on a Ru(II) Complex: Synthesis, Characterization, and Photoinduced Electron Transfer Reactions of $[Ru(TTF\text{-}dppz)_2(Aqphen)]^{2+}$

Nathalie Dupont,[†] Ying-Fen Ran,[‡] Hong-Peng Jia,[‡] Jakob Grilj,[†] Jie Ding,[†] Shi-Xia Liu,*[,‡] Silvio Decurtins,[‡] and Andreas Hauser*[,†]

[†]Département de Chimie Physique, Université de Genève, 30 Quai Ernest-Ansermet, CH-1211 Genève 4, Switzerland

[‡]Departement für Chemie und Biochemie, Universität Bern, Freiestrasse 3, CH-3012 Bern, Switzerland

Supporting Information

ABSTRACT: The synthesis and the photophysical properties of the complex $[Ru(TTF\text{-}dppz)_2(Aqphen)]^{2+}$ (TTF = tetrathiafulvalene, dppz = dipyrido-[3,2-*a*:2′,3′-*c*]phenazine, Aqphen = anthraquinone fused to phenanthroline via a pyrazine bridge) are described. In this molecular triad excitation into the metal−ligand charge transfer bands results in the creation of a long-lived charge separated state with TTF acting as electron donor and anthraquinone as terminal acceptor. The lifetime of the charge-separated state is 400 ns in dichloromethane at room temperature. A mechanism for the charge separation involving an intermediate charge-separated state is proposed based on transient absorption spectroscopy.

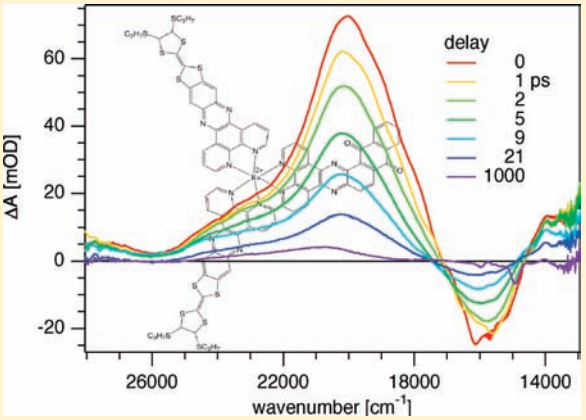

1. INTRODUCTION

There has been a considerable amount of research on the photophysical properties of metal complexes, in particular of ruthenium(II) complexes, containing bidentate ligands such as 2,2′-bipyridine (bpy) or 1,10-phenanthroline (phen) and their derivatives.[1−7] The interest in this type of complexes relies on their stability and use in multiple applications, as for instance in solar energy conversion[8−11] and molecular electronic devices.[12−14] A common feature of these complexes is their ability to absorb most of the visible light and thereby to access excited states by means of metal-to-ligand charge-transfer (MLCT) transitions. The well-known derivative of phen, dipyrido-[3,2-*a*:2′,3′-*c*]-phenazine (dppz) has two low-lying π^* acceptor levels, one localized on the phenazine subunit and one on the phenanthroline subunit of the molecule.[15] It is generally acknowledged that in the mixed ligand complex $[Ru(bpy)_2(dppz)]^{2+}$, the Ru(II)→bpy and Ru(II)→dppz ^{1}MLCT states are close to each other in energy, but the lowest emissive ^{3}MLCT state in solution is the Ru(II)→dppz state.[16]

Tetrathiafulavelene (TTF) can be fused to dppz to result in a TTF-dppz ligand (Scheme 1) with two redox centers and a lowest excited state corresponding to a TTF→dppz intraligand charge-transfer (^{1}ILCT) state, manifesting itself in a strong absorption band at 18700 cm^{-1} in CH_2Cl_2. The ligand on its own shows solvent dependent fluorescence centered at 12200 cm^{-1} with a large Stokes shift from its ^{1}ILCT state and a quantum efficiency of 0.01 (τ = 0.4 ns) in CH_2Cl_2.[17] The ruthenium(II) complexes of this ligand in the series $[Ru(bpy)_{1-n}(TTF\text{-}dppz)_n]^{2+}$, n = 1−3, also show interesting photophysical properties.[18] The ^{1}ILCT state shifts to lower energies by around 2000 cm^{-1} as a result of the coordination to ruthenium(II), and in addition to a weak luminescence attributed to the ^{1}ILCT state, they possess nonemissive but long-lived ($\tau \approx 2.4$ μs) charge-separated states. The latter correspond to an electron transfer from TTF to dppz, with the TTF and dppz moieties belonging to two different subunits, best formulated as $[Ru(L)(TTF^+\text{-}dppz)(TTF\text{-}dppz^-)]^{2+}$ with L = bpy or the third TTF-dppz for n = 2 and 3, respectively, resulting from the initial excitation into the ^{1}MLCT bands. The ^{3}MLCT luminescence in these cases is completely quenched by the reductive formation of the nonemissive state. For n = 1, the acceptor moiety for the charge separated state is provided by one of the bpy ligands. In this case, the ^{3}MLCT luminescence, although observed with a lower quantum efficiency than for the reference complex $[Ru(bpy)_2(dppz)]^{2+}$, has a longer lifetime of 1040 ns.[18] This can only be reconciled with the fact that depending upon which of the ^{1}MLCT transitions, Ru→bpy or

Received: September 23, 2010
Published: March 17, 2011

Scheme 1. (a) TTF-dppz, (b) Aqphen, and (c) $[Ru(TTF\text{-}dppz)_2(Aqphen)]^{2+}$ (**1**)

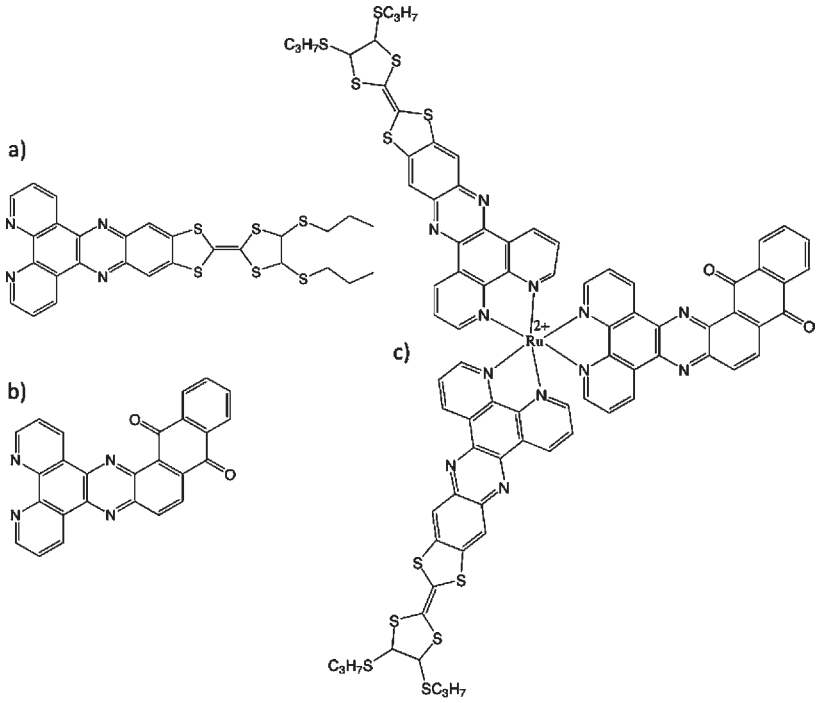

Ru→dppz, is excited two different relaxation paths are followed. For the former excitation, the above-mentioned formation of the charge separated state quenches the luminescence, for the latter, the electron sitting on the dppz unit of the only TTF-dppz ligand prevents electron transfer from TTF to the formal Ru^{3+}. As a result, the ^{3}MLCT state decays via the standard intrinsic decay accompanied by luminescence. In the related system, $[Ru(bpy)_2(TTF\text{-}ppb)]^{2+}$ with TTF-ppb = TTF-fused dipyrido-[2,3-*a*:3′,2′-*c*]phenazine, in which coordination of Ru(II) to the phenazine is side on, the MLCT to the ppb ligand occurs at substantially lower energy than the one to bpy. Therefore irradiation into the ^{1}MLCT band of bpy does not result in the corresponding ^{3}MLCT luminescence but in efficient relaxation to the MLCT state involving ppb. From there, the geometric proximity of the TTF moiety to the formal Ru^{3+} is proposed to allow a direct through space reductive quenching of the ^{3}MLCT luminescence via the ^{3}ILCT state of TTF-ppb.[19,20]

A famous electron acceptor is provided by quinones, widely studied because of their very important role in nature, as for instance in the photosystems of green plants. Anthraquinone can be fused to phenanthroline via a pyrazine bridge to form the Aqphen ligand shown in Scheme 1.[21,22] The combination of two TTF-dppz ligands and one Aqphen ligand to form a Ru(II) complex gives rise to the title complex $[Ru(TTF\text{-}dppz)_2(Aqphen)]^{2+}$ (**1**) also shown in Scheme 1. Its synthesis has been stimulated by the search for new antenna systems capable of charge separation[23] as well as for new photoredox switches.[24] So far only a few papers on Ru(II) coordination complexes with TTF derivatives have appeared in the literature.[18,20,25−30] In most cases, the famous luminescence from ^{3}MLCT states is strongly quenched by intramolecular electron transfer quenching from the pendant TTF unit. This makes them promising candidates for incorporation into optical sensors and devices. Herein we report the synthesis of Ru(II) complex **1** and thoroughly examine its electrochemical and photophysical properties. A direct comparison with the above-mentioned reference complex $[Ru(bpy)(TTF\text{-}dppz)_2]^{2+}$ indicates a new relaxation pathway in **1**.

2. EXPERIMENTAL METHODS

2.1. General Procedures. Unless otherwise stated, all reagents were purchased from commercial sources and used without additional purification. 5,6-Diamino-2-(4,5-bis(propylthio)-1,3-dithio-2-ylidene)-benzo[*d*][1,3]dithiole (TTF-diamine),[17] 12,17-dihydronaphtho-[2,3-*h*]dipyrido[3,2-*a*:2′,3′-*c*]-phenazine-12,17-dione (Aqphen)[21], and $[Ru(phendione)_2Cl_2]$[31] were prepared according to literature procedures. ^{1}H NMR spectra were obtained on a Bruker AC 300 spectrometer operating at 300.18 MHz: chemical shifts are reported in ppm referenced to residual solvent protons (CD_3CN and DMSO-d_6). The following abbreviations were used: s (singlet), d (doublet), t (triplet), m (multiplet), and br (broad). Infrared spectra were recorded on a Perkin-Elmer Spectrum One FT-IR spectrometer using KBr pellets. High-resolution mass spectra were recorded using a LTQ Orbitrap XL for Electrospray Ionization (ESI).

2.2. Synthesis. Synthesis of $[Ru(phendione)_2(Aqphen)](PF_6)_2$. In a Schlenk flask (25 mL), a solution of $[Ru(phendione)_2Cl_2]$ (208 mg, 0.35 mmol) and the ligand Aqphen (160 mg, 0.38 mmol) in ethylene glycol (16 mL) was heated at 195 °C for 14 h under Argon. After cooling down to room temperature, water (32 mL) was added into the resulting solution, and a black precipitate was immediately formed. After filtration, an excess of NH_4PF_6 (200 mg) was added to the filtrate. The resultant dark brown precipitate was isolated by suction filtration, washed with water, and dried in vacuum. The crude product was dissolved in CH_3CN (15 mL) and purified by precipitation with the addition of diethyl ether. After filtration, the analytically pure product was obtained as a black powder. Yield: 221 mg (51%). ^{1}H NMR (CD_3CN): δ = 7.55 (d, J = 6.0 Hz, 2H), 7.75 (m, 3H), 7.91−8.04 (m, 4H), 8.20−8.28 (m, 4H), 8.39 (br, 2H), 8.54 (br, 2H), 8.62 (d, J = 7.5 Hz, 2H), 8.75 (d, J = 8.4 Hz, 2H), 9.67 (d, J = 7.5 Hz, 2H), 9.76 (d, J = 7.8 Hz, 1H) ppm. IR (KBr): ν 1703, 1669, 1627, 1400, 1384, 1290, 843 cm^{-1}. ESI-MS: m/z 1079.0556, calcd.

dx.doi.org/10.1021/ic101951n |*Inorg. Chem.* 2011, 50, 3295–3303

Scheme 2. Synthesis of the Target Complex 1

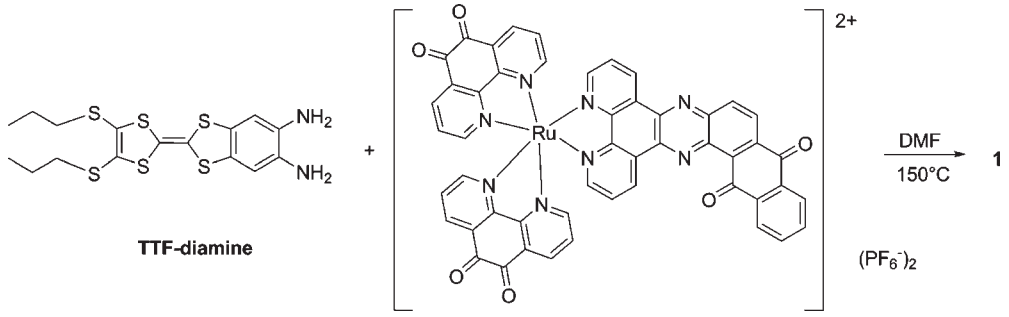

Table 1. Redox Potentials (V vs Ag/AgCl) of 1 in CH_2Cl_2 and of the Reference Compounds TTF-dppz,[17] Aqphen,[15] $[Ru(bpy)_2(TTF\text{-}dppz)]^{2+}$,[16] $[Ru(bpy)(TTF\text{-}dppz)_2]^{2+}$,[18] $[Ru(TTF\text{-}dppz)_3]^{2+}$,[18] and $[Ru(bpy)_2(Aqphen)]^{2+}$ [15]

	reduction				oxidation		
compound	$E_{1/2}^4$	$E_{1/2}^3$	$E_{1/2}^2$	$E_{1/2}^1$	$E_{1/2}^1$	$E_{1/2}^2$	$E_{1/2}^3$
1	−1.51[b]	−1.29[b]	−0.93[a,b]	−0.39[a,b]	0.79	1.14	1.48[a]
TTF-dppz		−1.17			0.73	1.08	
Aqphen[c]			−0.76	−0.46			
$[Ru(bpy)_2(TTF\text{-}dppz)]^{2+}$	−1.35	−0.91			0.74	1.05	1.43
$[Ru(bpy)(TTF\text{-}dppz)_2]^{2+}$	−1.50	−0.93			0.74	1.09	1.51
$[Ru(TTF\text{-}dppz)_3]^{2+}$		−0.86[b]			0.75	1.10	1.61
$[Ru(bpy)_2(Aqphen)]^{2+,c}$			−0.80	−0.18			1.24

[a] Quasi-reversible. [b] Glassy carbon working electrode at scan rate of 1 $V \cdot s^{-1}$. [c] In 1,2-dichloroethane

for $[M - PF_6^-]^+$: 1079.0493; 935.0983, calcd. for $[M + H - 2PF_6^-]^+$: 935.0941; 468.0532, calcd. for $[M + 2H - 2PF_6^-]^{2+}$: 468.0509.

Synthesis of $[Ru(TTF\text{-}dppz)_2(Aqphen)](PF_6)_2$. In a Schlenk flask (25 mL), a mixture of $[Ru(phendion)_2(Aqphen)](PF_6)_2$ (123 mg, 0.10 mmol) and 5,6-diamino-2-(4,5-bis(propylthio)-1,3-dithio-2-ylidene)-benzo[*d*][1,3]dithiole (87 mg, 0.20 mmol) in DMF (4 mL) was heated at 150 °C for 5 h under Argon. After cooling down to room temperature, water (5 mL) was added into the black solution. The resultant black powder was filtered off, washed with water, and dried in vacuum. The crude product was dissolved in CH_3CN (20 mL) and purified by chromatography on basic Al_2O_3 with CH_2Cl_2/MeOH (10:1) as eluent to afford the analytically pure product as a black powder. Yield: 23 mg (11%). ^1H NMR (DMSO-d_6): δ = 0.94 (t, J = 5.4 Hz, 12H), 1.62−1.66 (m, 8H), 2.91 (t, J = 5.4 Hz, 8H), 7.92−8.04 (m, 6H), 8.07 (d, J = 4.2 Hz, 1H), 8.09 (d, J = 4.2 Hz, 1H), 8.29 (d, J = 5.7 Hz, 2H), 8.34−8.37 (m, 4H), 8.39 (d, J = 4.5 Hz, 2H), 8.58 (s, 4H), 8.86 (dd, J = 6.6 Hz, J = 4.2 Hz, 2H), 9.55 (d, J = 6.3 Hz, 4H), 9.67 (d, J = 6.0 Hz, 1H), 9.76 (d, J = 6.0 Hz, 1H) ppm. IR (KBr): ν 2953, 2923, 1664, 1630, 1401, 1384, 1356, 1088, 841 cm^{-1}. ESI-HRMS: m/z 863.0177; calcd. for $[M - 2PF_6^-]^{2+}$: 863.0165. Anal. Calcd (%) for $C_{82}H_{56}F_{12}N_{12}O_2P_2RuS_{12} \cdot 5H_2O$: C, 46.74; H, 3.16; N, 7.98. Found: C, 46.67; H, 2.96; N, 7.59.

2.3. Physical Methods. Cyclic voltammetry was conducted on a VA-Stand 663 electrochemical analyzer. An Ag/AgCl electrode containing 2 M LiCl served as reference electrode, a glassy carbon electrode as counter electrode, and a Pt disk as working electrode. Cyclic voltammetric measurements were performed at room temperature under N_2 in CH_2Cl_2/CH_3CN (3:1) with 0.1 M Bu_4NPF_6 as supporting electrolyte at a scan rate of 100 $mV \cdot s^{-1}$. CH_2Cl_2 was filtered through basic alumina prior to use to avoid the presence of traces of H^+.

Photophysical measurements were performed on solutions of the compounds in CH_3CN and CH_2Cl_2 at room temperature. For luminescence and transient absorption measurements, the solutions were degassed by bubbling N_2 through them for 30 min. Absorption spectra were recorded on a Varian Cary 5000 UV/vis/near-IR (NIR) spectrophotometer. Excited state decay curves on the nanosecond time scale were recorded by exciting the samples at 458 nm using the third harmonic of a pulsed Nd:YAG laser (Quantel Brilliant) to pump an OPO (Opotek Magic Prism). The probe light came from a W-halogen lamp. The system used for detection consisted of a single monochromator (Spex 270 M), a photomultiplier (Hamamatsu R928), and a digital oscilloscope (Tektronix TDS 540B). The overall time resolution is ~15 ns. Corresponding transient absorption spectra were recorded with a gated CCD camera (Andor iStar 720).

The femtosecond transient absorption setup has been described elsewhere.[32] Briefly, the output of a Ti:sapphire amplifier (Spitfire, Spectra Physics; 800 nm pulses of 150 fs FHWM) is split into two parts; about 5 μJ are focused into a 3 mm thick, constantly moving CaF_2 window to generate a white light continuum for probing, the remainder is sent into a home-built two stage noncollinear optical parametric amplifier to generate the pump pulses at 400 nm or at 650 nm. The polarization of the pump beam is set to magic angle with respect to the probe beam. The pump power at the sample is approximately 0.1 mJ/cm^2. The sample solution in a 1 mm quartz cell is constantly stirred by nitrogen bubbling. The photochemical stability of the sample is verified by the steady state absorption spectrum. The probe beam is dispersed in a spectrograph (Andor, SLR163) and imaged onto a 512 × 58 pixel back-thinned CCD (Hamamatsu S07030−09). The spectra are corrected for the chirp of the white light pulses by standard procedures.[33] The IRF (as deduced from the electronic OKE signal) has a FHWM of approximately 200 fs, depending on the wavelength. Because of cross-phase-modulation and the coherent signal, the spectra at early time-delays cannot be observed.

3. RESULTS AND DISCUSSION

3.1. Synthesis and Characterization. To circumvent the solubility problems that are often encountered when

dx.doi.org/10.1021/ic101951n |*Inorg. Chem.* 2011, 50, 3295–3303

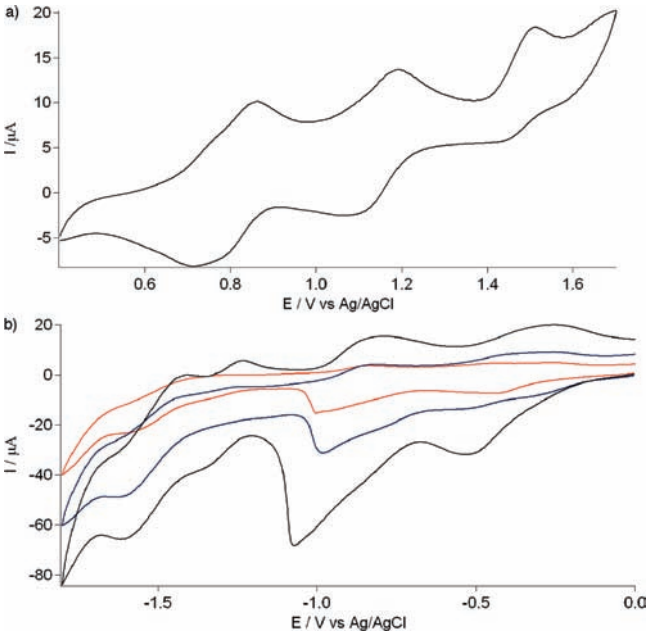

Figure 1. Cyclic voltammograms of **1** (5×10^{-4} M) in CH_2Cl_2/CH_3CN (3:1) (0.1 M $TBAPF_6$ (TBA = tetrabutylammonium): (a) with positive potentials between 0.4 and 1.7 V using a platinum disk working electrode; scan rate 100 mV·s^{-1}) ; (b) with negative potentials between 0 and −1.7 V using a glassy carbon working electrode; at different scan rates (100 mV·s^{-1}, red; 500 mV·s^{-1}, blue; 1 V·s^{-1}, black).

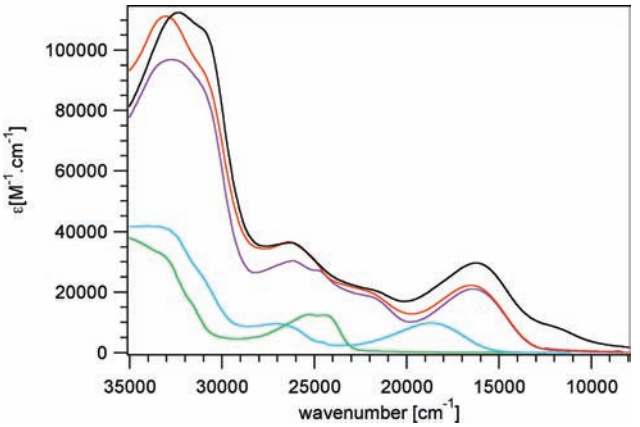

Figure 2. Absorption spectra of TTF-dppz (blue), Aqphen (green), $[Ru(bpy)(TTF\text{-}dppz)_2]^{2+}$ (purple), $[Ru(TTF\text{-}dppz)_3]^{2+}$ (black), and **1** (red) in CH_2Cl_2 at room temperature.

incorporating rigid and planar diimine ligands into extended mononuclear and polynuclear Ru(II) systems, a synthetic approach to the target Ru(II) complex **1** involves direct condensation of a TTF-diamine ligand with $[Ru(phendione)_2(Aqphen)]^{2+}$ (Scheme 2). The latter was obtained in reasonable yield by a reaction of $[Ru(phendione)_2Cl_2]$ with 1.1 equiv of Aqphen in ethylene glycol at reflux. Both new Ru(II) compounds were purified by recrystallization or by chromatographic separation on basic Al_2O_3. Spectroscopic characterization (^{1}H NMR, IR and ESI-HRMS data in the Experimental Section) confirmed the formation of the desired complexes.

3.2. Electrochemistry. The electrochemical properties of **1** were investigated by cyclic voltammetry. The electrochemical data are collected in Table 1 together with those of $[Ru(bpy)_2(TTF\text{-}dppz)]^{2+}$, $[Ru(bpy)(TTF\text{-}dppz)_2]^{2+}$, $[Ru(TTF\text{-}dppz)_3]^{2+}$, $[Ru(bpy)_2(Aqphen)]^{2+}$, TTF-dppz, and Aqphen, for comparison. As illustrated in Figure 1a, complex **1** undergoes two reversible multielectron oxidation processes for the oxidation of the two TTF fragments. Compared to the free ligand TTF-dppz, the observed redox potentials of **1** for the TTF oxidation processes are slightly positive-shifted because of the electrostatic inductive effect of the Ru(II) ion bound to the imine-chelating units. Besides, one quasi-reversible oxidation wave, corresponding to the Ru(II/III) redox couple, was observed. The influence of the electron withdrawing ligands is nicely expressed by the values of the half wave potentials of the Ru(II/III) couple of the complexes given in Table 1. In the series $[Ru(bpy)_{3-n}(TTF\text{-}dppz)_n]^{2+}$, $n = 1-3$, the potential increases with n. This is due to the electron withdrawing properties of the increasing number of TTF moieties oxidized before the oxidation of Ru(II). In the title complex **1**, one of the three ligands is Aqphen, which in its neutral form is less electron withdrawing than a dppz-$TTF^{+\bullet}$ radical. As a result, the Ru(II/III) potential of **1** is close to the one for $n = 2$.

In the cathodic region, complex **1** displays several reduction waves. Several cyclic voltammetry (CV) measurements have been performed at different scan rates (see Supporting Information) using a Pt disk working electrode. On the one hand, the peak-to-peak separations ($\Delta E_p = E_{pa} - E_{pc}$) increase at high scan rates, indicating a quasi-reversible nature of the electron-transfer processes for the reduction of the quinone moiety of Aqphen and the dppz units. On the other hand, the intensities of the reduction waves decrease, and concomitantly all reduction processes become irreversible as the potentials are cycled. It can be therefore deduced that the semiquinone and hydroquinone species in the vicinity of the working electrode appear to be quite unstable. For comparison, CV measurements of complex **1** were further performed at different scan rates using glassy carbon electrodes as counter and working electrodes (Figure 1b), for which the redox potentials are only slightly different from those using a Pt working electrode (see Supporting Information). However, the reversibility of the reduction waves becomes much more apparent with increasing scan rates. Complex **1** thus displays two quasi-reversible reduction waves at −0.39 and −0.93 V as well as two reversible waves at −1.29 and −1.51 V, which can be assigned to reductions of the quinone moiety of Aqphen and the different dppz units, respectively. Upon coordination, the first reduction potential of the Aqphen unit is slightly shifted to a less negative potential. However, this shift is less pronounced than for the reference complex $[Ru(bpy)_2(Aqphen)]^{2+}$ because of the donating properties of the TTF-dppz ligands. In contrast, the negative shift in the dppz-centered reduction in comparison to $[Ru(bpy)(TTF\text{-}dppz)_2]^{2+}$ is attributable to the presence of the previously reduced quinone unit in **1**. We may thus conclude that the overall lowest unoccupied molecular orbital (LUMO) in **1** resides on the quinone unit of Aqphen.

3.3. Photophysical Properties. The absorption spectra of **1** in CH_2Cl_2, together with those of $[Ru(bpy)(TTF\text{-}dppz)_2]^{2+}$, $[Ru(TTF\text{-}dppz)_3]^{2+}$, TTF-dppz, and Aqphen are presented in Figure 2. By comparison with the spectra of the free ligands and the reference complexes, the absorption bands of **1** can be readily attributed to specific transitions. The broad absorption band at 16500 cm^{-1} corresponds to the ^{1}ILCT transition

dx.doi.org/10.1021/ic101951n |*Inorg. Chem.* 2011, 50, 3295–3303

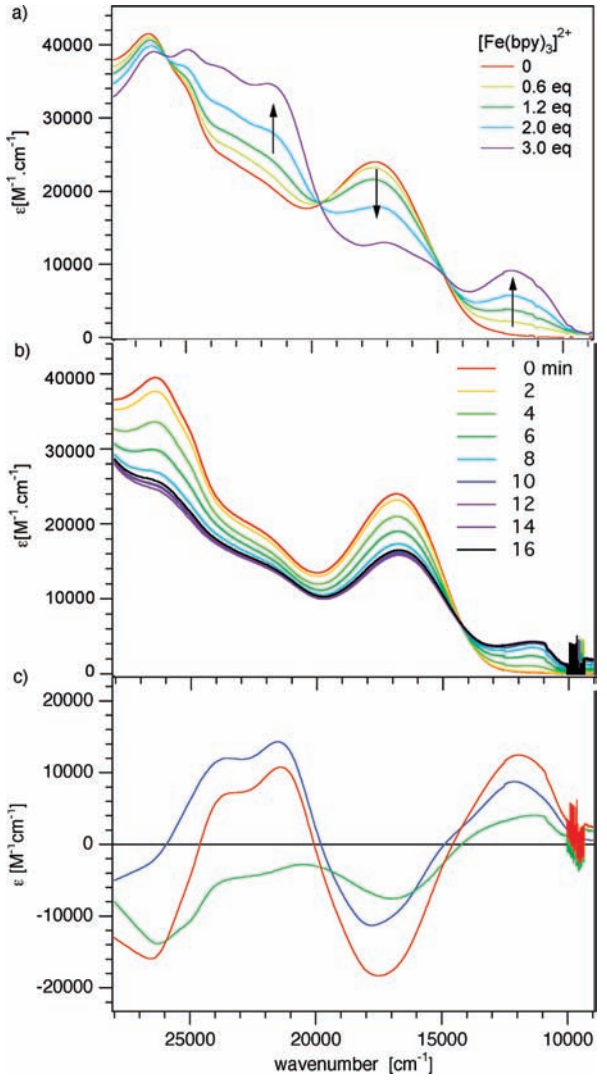

Figure 3. UV−vis spectra of **1** during (a) Chemical oxidation in CH_3CN as a function of equivalents of $[Fe(bpy)_3]^{3+}$ added to the solution. The spectra are corrected for the generated $[Fe(bpy)_3]^{2+}$. (b) Electro-chemical reduction at −0.50 V vs Ag/AgCl in CH_2Cl_2 at room temperature, cell: 0.7 mm. (c) Difference spectra, (blue) oxidized form − neutral form, (green) reduced form − neutral form, (red) oxidized form + reduced form − 2×neutral form.

occurring on the TTF-dppz ligands, as shown previously for the series of reference complexes $[Ru(bpy)_{3-n}(TTF\text{-}dppz)_x]^{2+}$, n = 1−3,[18] with the TTF subunit acting as an electron donor, while dppz is acting as an electron acceptor. With respect to the free ligand this ^{1}ILCT absorption band is red-shifted by 2000 cm^{-1}, corresponding to a lowering of the energy of the unoccupied molecular orbital located on the dppz subunit because of the coordination to ruthenium(II). As expected, the extinction coefficient of the ^{1}ILCT absorption band on TTF-dppz increases from 1×10^4 to 2.2×10^4 M^{-1} cm^{-1} upon coordination of two TTF-dppz subunits and one Aqphen subunit to ruthenium(II). By comparison with the reference complexes,[18] the electric-dipole-allowed $Ru^{2+}\rightarrow$dppz ^{1}MLCT transition is located at around 21900 cm^{-1}. The corresponding $Ru^{2+}\rightarrow$phen ^{1}MLCT transition to the Aqphen ligand is located at roughly the same energy. The absorption band centered at 26500 cm^{-1} can be

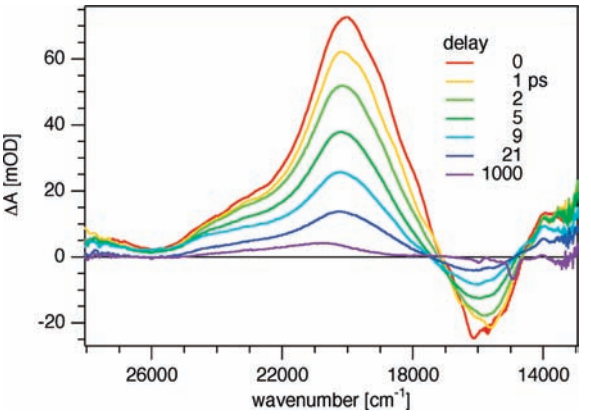

Figure 4. Transient absorption spectra of $[Ru(TTF\text{-}dppz)_2(Aqphen)]^{2+}$ at room temperature in CH_2Cl_2 on the ps time scale with an excitation wavelength of 650 nm (excitation in the ^{1}ILCT band).

assigned to the $\pi-\pi^*$ transitions located on the dppz subunits in both TTF-dppz as well as in Aqphen. In the UV region, a broad band is attributed to $\pi-\pi^*$ transitions located on the different subunits. Similar to $[Ru(TTF\text{-}dppz)_3]^{2+}$ and $[Ru(bpy)(TTF\text{-}dppz)_2]^{2+}$,[18] no luminescence from any ^{3}MLCT state of **1** could be detected in the limit of the sensitivity of the experimental setup. In contrast to the TTF-dppz and its complexes,[18] for which weak luminescence from the ^{1}ILCT state of TTF-dppz was observed, **1** does not show any luminescence from that state either.

Upon chemical oxidation (Figure 3a) of **1** with $[Fe(bpy)_3]^{3+}$ in CH_3CN, the ^{1}ILCT absorption band located at 17500 cm^{-1} decreases in intensity and two new bands appear at 12000 and 21500 cm^{-1}, respectively, the one at higher energy being more intense. In analogy to the previous study of TTF-dppz and its complexes,[18] the new absorption spectrum highlights the oxidation of the TTF subunit, and in particular, the new absorption band in the near IR in turn corresponds to an inverse dppz$\rightarrow$TTF$^{\bullet+1}$ ILCT transition. This oxidation seems to be irreversible chemically.

Likewise, **1** can be reduced by a one-electron reduction at −0.50 V vs Ag/AgCl. The corresponding spectra as a function of time are shown in Figure 3b. The overall effect of the reduction on the absorption spectrum is less pronounced compared to the oxidation. There is a small decrease in the intensity of the ^{1}ILCT band and a weak absorption at 12000 cm^{-1}, but in the region of the strong absorption of the oxidized form there is only a general overall decrease in the absorption intensity. This is further illustrated by the difference spectra in Figure 3c.

To arrive at a better understanding of the photophysical behavior of **1** and the role of the Aqphen ligand in the molecule, compared to the reference complex $[Ru(bpy)(TTF\text{-}dppz)_2]^{2+}$, transient absorption spectra were recorded on different time scales using different excitation wavelengths. Figure 4 shows the transient difference absorption spectrum of **1** on the ps time scale upon excitation at 650 nm (15400 cm^{-1}), that is, into the ^{1}ILCT band. The initial bleaching of the band at 15800 cm^{-1} and the strong absorption at 20000 cm^{-1} immediately following the laser pulse (nominally at t = 0) are signatures of the ^{1}ILCT state.

This signal decays quite rapidly, but the actual decay curves extracted from the spectra and shown at different wavelengths in Figure 5a are not monoexponential. A global fit with a the sum of two exponentials yields a satisfactory fit with τ_1 = 4.7(5) ps and

dx.doi.org/10.1021/ic101951n |Inorg. Chem. 2011, 50, 3295–3303

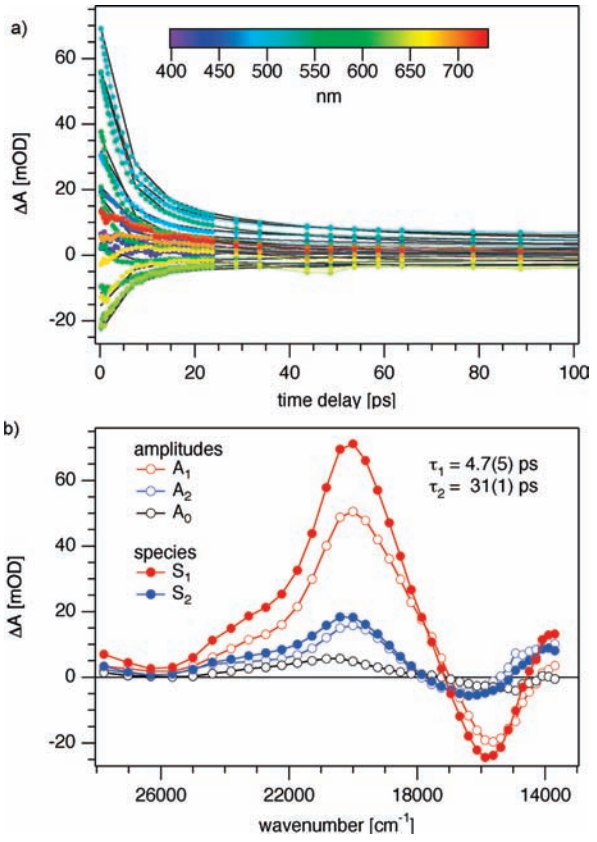

Figure 5. (a) Global fit to the transient absorption spectra of Figure 4 with a double exponential decay resulting in a decay rate constant of $2.1(2) \times 10^{11}$ s^{-1} (τ = 4.7(5) ps). (b) Amplitudes of the double exponential fit as a function of wavelength.

τ_2 = 31(1) ps. The corresponding amplitudes as a function of wavelength are shown in Figure 5b. The amplitude of the longer lifetime, A_2, is considerably smaller than the one of the shorter one, A_1. We thus interpret τ_1 as being the lifetime of the ^{1}ILCT, which for the most part decays in a radiationless process directly to the ground state, and τ_2 as being the lifetime of a minority intermediate species, the nature of which is not clear at this stage, populated from the initially excited state and decaying likewise to the ground state. In this case A_1 is close to the difference spectrum between the initially excited state and the ground state, and A_2 to the one between the intermediate state of the minority relaxation pathway and the ground state. The small residual amplitude, A_0, is probably due to photochemical degradation during the experiment, as a nanosecond experiment on a freshly prepared sample with irradiation into the ^{1}ILCT band gave no transient signals on the nanosecond time scale or longer (Supporting Information, Figure S2).

Figure 6 shows the transient absorption spectrum of **1** likewise on the ps time scale upon excitation at 400 nm (25000 cm^{-1}), that is, into the ^{1}MLCT absorption bands. The initial spectrum (at nominally t = 0) shows a strong excited state absorption with a maximum at 20200 cm^{-1} and no bleaching at any wavelength. The time evolution of the transient spectrum is clearly not single exponential. The band at 20200 cm^{-1} decays within ~40 ps and is replaced by a double hump with maxima at 20600 and 22500 cm^{-1}, and a weak bleaching is observed at 16000 cm^{-1}. This spectrum further evolves with an increasing intensity, a shift

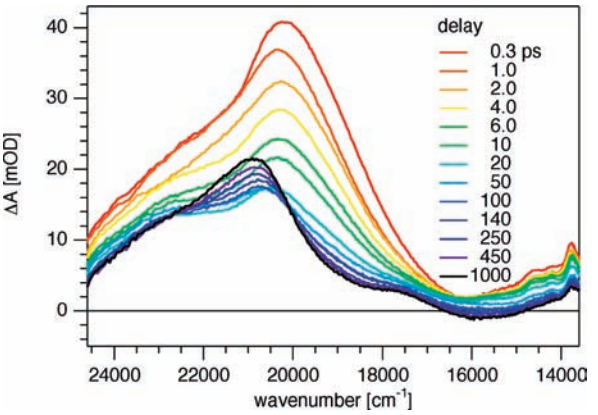

Figure 6. Transient absorption spectra of $[Ru(TTF\text{-}dppz)_2(Aqphen)]^{2+}$ at room temperature in CH_2Cl_2 on the ps time scale with an excitation wavelength of 400 nm (excitation in the ^{1}MLCT bands).

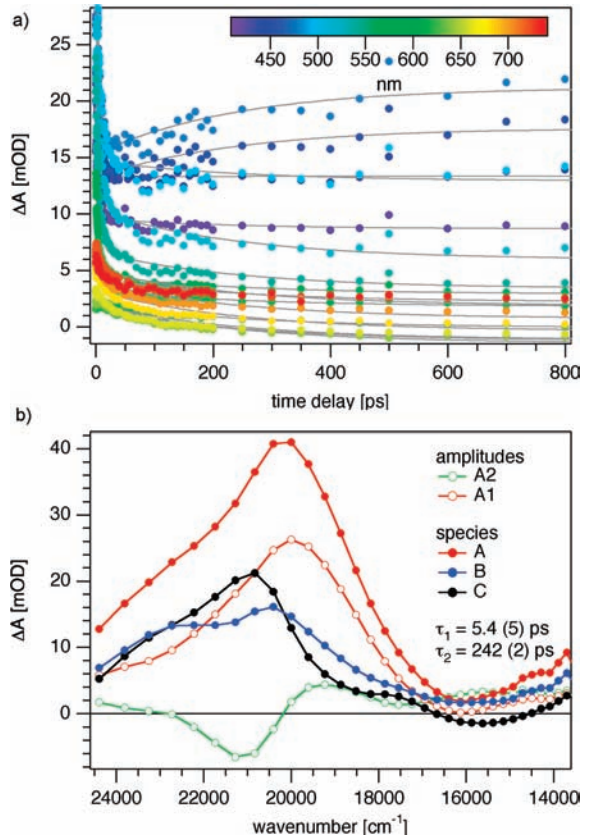

Figure 7. Global fit of a double exponential decay and an offset to the data in Figure 6: (a) experimental decay curves and corresponding fits at different wavelengths, (b) amplitudes (A_1 and A_2) and synthesized difference spectra of the transient species in the proposed sequence A→B→C as function of wavelength.

of the maximum to 21000 cm^{-1}, and an increased bleaching at 16000 cm^{-1}. This final spectrum persists to beyond 1 ns. We may interpret this as an A→B→C sequence occurring within the first nanosecond after the excitation.

The global fit with a double exponential shown in Figure 7a indeed clearly identifies two time constants, namely, a fast process with τ_1 = 5.4(5) ps ($k_1 = 1.8(2) \times 10^{11}$ s^{-1}) and a

dx.doi.org/10.1021/ic101951n |*Inorg. Chem.* 2011, 50, 3295–3303

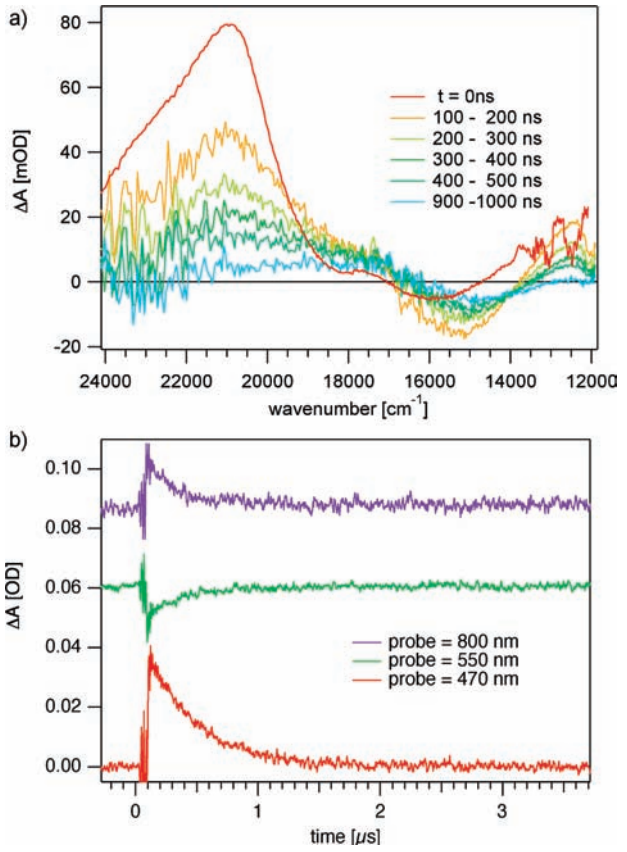

Figure 8. (a) Transient absorption spectrum of **1** in CH_2Cl_2 integrated over 100 ns in 100 ns intervals after pulsed irradiation at 458 nm, for direct comparison the last spectrum from Figure 6 is included, (b) decay curves on the μs time scale at 470 nm (21300 cm^{-1}) and 550 nm (18200 cm^{-1}) and 800 nm (12500 cm^{-1}).

slower process with τ_2 = 242(2) ps (k_2 = 4.1(2) × 10^9 s^{-1}). Because the two time constants are very much different, the characteristic difference absorption spectra for the initially excited state (A), the intermediate state (B), and the final state (C) can be synthesized from the corresponding amplitudes (A_1 and A_2) and the offset (A_0 = C) all shown in Figure 7b. A is very similar to the first spectrum, B to the one at $t \approx 40$ ps, and the offset to the last spectrum in Figure 6. By comparison with the difference spectra of the oxidized and reduced forms of **1** (Figure 3), spectrum C with a maximum at 21000 cm^{-1} having a shoulder on the high energy side and a weak bleaching at 16000 cm^{-1} can be attributed to the formation of a cationic $TTF^{\bullet+}$ subunit in conjunction with a neutral dppz moiety.[17] This implies a long-lived charge-separated excited state reached by photoexcitation at 400 nm, the question we will try to answer below being where is the odd electron localized.

In a last step, the decay of the signal persisting to beyond 1 ns was investigated by transient absorption spectroscopy on the nano to microsecond time scale. The corresponding spectra are shown in Figure 8 for **1** in CH_2Cl_2 upon excitation at 458 nm (21800 cm^{-1}), that is, as before into the ^{1}MLCT transitions of the complex. Besides a bleaching of the ^{1}ILCT ground state absorption band at 16000 cm^{-1}, there are two transient absorption bands at 21000 and 12500 cm^{-1}, respectively, that is, at the same energies as for the residual spectrum of the ps experiment with irradiation at 400 nm. The corresponding transient state has

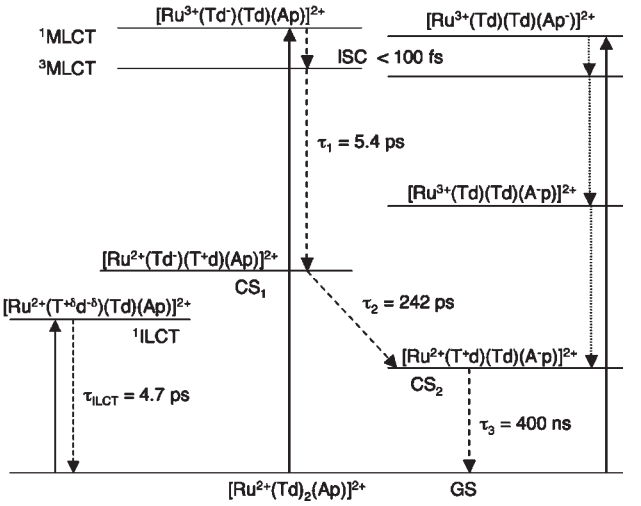

Figure 9. Energy level scheme for $[Ru(TTF\text{-}dppz)_2(Aqphen)]^{2+}$; the most probable pathway for the creation of the low-energy charge-separated state via excitation into the ^{1}MLCT band to dppz on TTF-dppz is shown by broken lines, an alternative pathway for excitation into the ^{1}MLCT band to phen on Aqphen by dotted lines (Notation: TTF → T, dppz → d, Aq → A, phen → p).

a lifetime of approximately 400 ns in CH_2Cl_2 at room temperature as exemplified by the decay curves recorded at three different probe wavelengths shown in Figure 8b.

In summary, following initial excitation into the ^{1}ILCT band at 650 nm (15400 cm^{-1}) results in a transient signal which majoritarily decays to the ground state with a lifetime of 4.7(5) ps. This is thus the lifetime of the ^{1}ILCT state in the complex. A minority pathway results in a small concentration of an intermediate species with a somewhat longer lifetime having a very similar transient spectrum. Following excitation into the ^{1}MLCT bands at 400 or 458 nm, the relaxation occurs in three steps: first to an intermediate state with a time constant τ_1 of 5.4 ps. The intermediate state, in turn, leads to a charge separated state with a time constant τ_2 of 242 ps. Finally, the charge-separated state has a lifetime τ_3 of 400 ns.

Using spectroscopic and CV data, the energy level scheme shown in Figure 9 can be constructed. The spectroscopically accessible ^{1}MLCT states for both ligands are approximately at the same energy of around 2.5 eV (20200 cm^{-1}), with the one involving Aqphen at slightly lower energy because of the electron withdrawing effect of anthraquinone as opposed to the electron donating effect of TTF. As for all ruthenium(II) polypyridyl complexes, the corresponding ^{3}MLCT states are expected to be at around 0.4 eV lower energies,[34] that is, at around 2.1 eV (17000 cm^{-1}). Upon excitation into the ^{1}MLCT bands, intersystem crossing on the femtosecond time scale takes the complexes to the corresponding ^{3}MLCT states.[35] This is not resolved in our spectra. Because there are two TTF-dppz and only one Aqphen ligands coordinated to ruthenium(II), excitation in the region of the ^{1}MLCT absorption bands creates a species formulated best as $[Ru^{3+}(TTF\text{-}dppz^-)(TTF\text{-}dppz)(Aqphen)]^{2+}$ as majority species, the ^{3}MLCT state of which therefore dominates the spectrum at t = 0 in Figure 6. The ^{3}MLCT luminescence being completely quenched, we must conclude that this species is very short-lived and decays to an intermediate state which is likewise nonemissive in an efficient nonradiative process. The second TTF-dppz can be expected to provide an electron and reestablish

dx.doi.org/10.1021/ic101951n |*Inorg. Chem.* 2011, 50, 3295–3303

the +2 charge on ruthenium, thus resulting in a first charge separated state (CS_1) formulated $[Ru^{2+}(TTF\text{-}dppz^{-})(TTF^{+}\text{-}dppz)(Aqphen)]^{2+}$, in analogy to the reference complex $[Ru(bpy)(TTF\text{-}dppz)_2]^{2+}$ briefly reviewed in the introduction.[18] From the redox potentials of the reference complex (Table 1), this state is at an estimated energy of 1.67 eV (13500 cm^{-1}). We attribute the 5.4 ps transient signal to this process. In the reference complex, that is, in the absence of any further acceptors, this charge-separated state has a lifetime of 2.4 μs. In the title complex **1**, the Aqphen acts as comparatively strong electron acceptor, thus instead of relaxing to the ground state, electron transfer from $dppz^{-}$ to the Aqphen takes place, resulting in the long-lived charge separated state $[Ru^{2+}\text{-}(TTF^{+}\text{-}dppz)(TTF\text{-}dppz)(Aq^{-}phen)]^{2+}$ (CS_2), that is, with the odd electron localized on the quinone part of Aqphen. From the difference in the corresponding redox potentials of **1** (Table 1) this state is located at 1.18 eV (9500 cm^{-1}). We attribute the 242 ps transient signal with the build up of a new species to this process, the driving force being 0.5 eV (4000 cm^{-1}). This state in turn decays to the ground state with a lifetime of 400 ns.

Of course excitation in the region of the ^{1}MLCT bands creates the corresponding ^{3}MLCT state with the electron on the phen unit of Aqphen to be formulated as $[Ru^{3+}(TTF\text{-}dppz)_2\text{-}(Aqphen^{-})]^{2+}$ as minority species.[15] This state has a very short lifetime as the electron density is redistributed to the quinone part of the ligand on the femtosecond time scale,[36] and subsequent electron transfer from TTF directly results in the final charge separated state most probably within the same 5.4 ps as the analogue process for the majority species.

A few questions still need answers: why is the lifetime of the charge-separated state CS_2 with the very good acceptor shorter than the one of the reference compound? Two reasons come to mind: (a) the charge recombination is in the Marcus inverted region and thus is faster for the smaller energy gap, (b) the Aqphen ligand is bent and thus through space interaction increases the electronic coupling. The latter could be tested by using the linear analogue of Aqphen as electron-accepting ligand. Furthermore, can we rule out that the 400 ns lifetime really is due to the CS_2 state and does not, as proposed for the side on coordination of the complex $[Ru(bpy)_2(TTF\text{-}ppb)]^{2+}$ reviewed in the introduction, correspond to the lifetime of the ^{3}ILCT?[19,20] On the basis of the present data, we perhaps cannot entirely rule it out, but by comparison of the transient spectra of $[Ru(bpy)_2(TTF\text{-}ppb)]^{2+}$ and $[Ru(bpy)(TTF\text{-}dppz)_2]^{2+}$ with those of the title compound a charge separated state is more likely.

Finally, for excitation into the ^{1}ILCT state even though it majoritarily decays to the ground state because of its intrinsic short lifetime, what is the minority transient species with a lifetime of 31 ps? From an energetic point of view a radiationless process in the form of an intramolecular energy transfer or charge transfer process could take the complex to the charge separated state. However, the driving force is smaller, and mechanistically this seems less probable than the other proposed transitions. Of course this would be the singlet CS_2 state as compared to the triplet CS_1 and CS_2 states created from the ^{3}MLCT states and would therefore have a shorter lifetime. At this stage it is, however, not clear how spin selection rules influence the different relaxation processes. Also overlapping absorption bands of course make it difficult to target a single excited state with the laser pulse.

4. CONCLUSIONS

The title complex, $[Ru(TTF\text{-}dppz)_2(Aqphen)]^{2+}$, constitutes a triad of chromophores engineered for directional light-induced electron transfer. The donor (TTF-dppz) and the acceptor (Aqphen) ligands are held together by the metal center. The latter, together with the ligating chromophores, acts as sensitizer via ^{1}MLCT transitions. The majority pathway for the creation of the long-lived light-induced charge-separated state, CS_2, involves several steps with an intermediate state, which is also a charge-separated state CS_1. In the absence of the final acceptor Aqphen, the CS_1 state would in turn be long-lived as observed in the reference complex $[Ru(bpy)(TTF\text{-}dppz)_2]^{2+}$.[18] In the reference complex, the light-induced electron transfer is not directional. In contrast, in the title complex the light-induced electron transfer is directional, and this constitutes an important property for potential applications in solar energy conversion and signal processing. In a next step, systems with different quinone based terminal acceptor ligands are to be investigated to establish how geometric effects influence the relaxation pathway. Likewise, minority pathways in particular taking into consideration spin selection rules and the influence of pH will have to be discussed in more detail.

■ ASSOCIATED CONTENT

Supporting Information. Cyclic voltammograms of **1** and nanosecond pulsed excitation upon excitation into the ^{1}ILCT band (PDF). This material is available free of charge via the Internet at http://pubs.acs.org.

■ AUTHOR INFORMATION

Corresponding Author

*E-mail: andreas.hauser@unige.ch (A.H.), liu@iac.unibe.ch (S.-X.L.).

■ ACKNOWLEDGMENT

This work was supported by the Swiss National Science Foundation (Grants 200020-125175 and 200020-130266/1) and EU(FUNMOLS FP7-212942-1). We thank E. Vauthey for helping us with his expertise in ultrafast spectroscopy.

■ REFERENCES

(1) Crosby, G. A. *Acc. Chem. Res.* **1975**, *8*, 231–238.
(2) Rusanova, J.; Decurtins, S.; Rusanov, E.; Stoeckli-Evans, H.; Delahaye, S.; Hauser, A. *J. Chem. Soc., Dalton Trans.* **2002**, 4318–4320.
(3) Delahaye, S.; Loosli, C.; Liu, S. X.; Decurtins, S.; Labat, G.; Neels, A.; Loosli, A.; Ward, T. R.; Hauser, A. *Adv. Funct. Mater.* **2006**, *16*, 286–295.
(4) Spiccia, L.; Deacon, G. B.; Kepert, C. M. *Coord. Chem. Rev.* **2004**, *248*, 1329–1341.
(5) Kozlov, D. V.; Tyson, D. S.; Goze, C.; Ziessel, R.; Castellano, F. N. *Inorg. Chem.* **2004**, *43*, 6083–92.
(6) Galletta, M.; Puntoriero, F.; Campagna, S.; Chiorboli, C.; Quesada, M.; Goeb, S.; Ziessel, R. *J. Phys. Chem. A* **2006**, *110*, 4348–58.
(7) Vos, J. G.; Kelly, J. M. *J. Chem. Soc., Dalton Trans.* **2006**, 4869–4883.
(8) Meyer, T. J. *Pure Appl. Chem.* **1986**, *58*, 1193–1206.
(9) Meyer, T. J. *Acc. Chem. Res.* **1989**, *22*, 163–170.
(10) Gu, J.; Chen, J.; Schmehl, R. H. *J. Am. Chem. Soc.* **2010**, *132*, 7338–7346.

(11) Alstrum-Acevedo, J. H.; Brennaman, M. K.; Meyer, T. J. *Inorg. Chem.* **2005**, *44*, 6802–6827.
(12) Balzani, V.; Gomez-Lopez, M.; Stoddart, J. F. *Acc. Chem. Res.* **1998**, *31*, 405–414.
(13) Handy, E. S.; Pal, A. J.; Rubner, M. F. *J. Am. Chem. Soc.* **1999**, *121*, 3525–3528.
(14) Gao, F. G.; Bard, A. J. *J. Am. Chem. Soc.* **2000**, *122*, 7426–7427.
(15) Lopez, R.; Leiva, A. M.; Zuloaga, F.; Loeb, B.; Norambuena, E.; Omberg, K. M.; Schoonover, J. R.; Striplin, D.; Devenney, M.; Meyer, T. J. *Inorg. Chem.* **1999**, *38*, 2924–2930.
(16) Delgadillo, A.; Arias, M.; Leiva, A. M.; Loeb, B.; Meyer, G. J. *Inorg. Chem.* **2006**, *45*, 5721–5723.
(17) Jia, C.; Liu, S. X.; Tanner, C.; Leiggener, C.; Neels, A.; Sanguinet, L.; Levillain, E.; Leutwyler, S.; Hauser, A.; Decurtins, S. *Chem.—Eur. J.* **2007**, *13*, 3804–3812.
(18) Goze, C.; Leiggener, C.; Liu, S. X.; Sanguinet, L.; Levillain, E.; Hauser, A.; Decurtins, S. *ChemPhysChem* **2007**, *8*, 1504–12.
(19) Goze, C.; Dupont, N.; Beitler, E.; Leiggener, C.; Jia, H.; Monbaron, P.; Liu, S. X.; Neels, A.; Hauser, A.; Decurtins, S. *Inorg. Chem.* **2008**, *47*, 11010–11017.
(20) Leiggener, C.; Dupont, N.; Liu, S. X.; Goze, C.; Decurtins, S.; Beitler, E.; Hauser, A. *Chimia* **2007**, *61*, 621–625.
(21) Lopez, R.; Loeb, B.; Boussie, T.; Meyer, T. J. *Tetrahedron Lett.* **1996**, *37*, 5437–5440.
(22) Arias, M.; Concepcion, J.; Crivelli, I.; Delgadillo, A.; Diaz, R.; Francois, A.; Gajardo, F.; Lopez, R.; Leiva, A. M.; Loeb, B. *Chem. Phys.* **2006**, *326*, 54–70.
(23) Wu, H.; Zhang, D. Q.; Su, L.; Ohkubo, K.; Zhang, C. X.; Yin, S. W.; Mao, L. Q.; Shuai, Z. G.; Fukuzumi, S.; Zhu, D. B. *J. Am. Chem. Soc.* **2007**, *129*, 6839–6846.
(24) Fang, C. J.; Zhu, Z.; Sun, W.; Xu, C. H.; Yan, C. H. *New J. Chem.* **2007**, *31*, 580–586.
(25) Campagna, S.; Serroni, S.; Puntoriero, F.; Loiseau, F.; De Cola, L.; Kleverlaan, C. L.; Becher, J.; Sorensen, A. P.; Hascoat, P.; Thorup, N. *Chem.—Eur. J.* **2002**, *8*, 4461–4469.
(26) Bryce, M. R. *Adv. Mater.* **1999**, *11*, 11–23.
(27) Goze, C.; Liu, S. X.; Leiggener, C.; Sanguinet, L.; Levillain, E.; Hauser, A.; Decurtins, S. *Tetrahedron* **2008**, *64*, 1345–1350.
(28) Keniley, L. K.; Ray, L.; Kovnir, K.; Dellinger, L. A.; Hoyt, J. M.; Shatruk, M. *Inorg. Chem.* **2010**, *49*, 1307–1309.
(29) Vacher, A.; Barriere, F.; Roisnel, T.; Lorcy, D. *Chem. Commun.* **2009**, 7200–7202.
(30) Pointillart, F.; Le Gal, Y.; Golhen, S.; Cador, O.; Ouahab, L. *Inorg. Chem.* **2008**, *47*, 9730–9732.
(31) Goss, C. A.; Abruna, H. D. *Inorg. Chem.* **1985**, *24*, 4263–4267.
(32) Duvanel, G.; Banerji, N.; Vauthey, E. *J. Phys. Chem. A* **2007**, *111*, 5361–5369.
(33) Yamaguchi, S.; Hamaguchi, H. O. *Appl. Spectrosc.* **1995**, *49*, 1513–1515.
(34) Juris, A.; Balzani, V.; Barigelletti, F.; Campagna, S.; Belser, P.; von Zelewsky, A. *Coord. Chem. Rev.* **1988**, *84*, 85–277.
(35) Tarnovsky, A. N.; Gawelda, W.; Johnson, M.; Bressler, C.; Chergui, M. *J. Phys. Chem. B* **2006**, *110*, 26497–26505.
(36) Lünnemann, S.; Kuleff, A. I.; Cederbaum, L. S. *J. Chem. Phys.* **2009**, *130*, 154305.